Chapter 5: Mechanical and biological behaviour of porous Ti-SiO2 scaffold for tissue engineering application

5.1.Introduction

Orthopaedic prostheses have shown continuous success in restoring the function of hard tissue and offering a high quality of life to millions of individuals. Therefore, the design and development of artificial bones and implants for replacement of injured/diseased hard tissues are highly desired for orthopaedic applications. Thus, the orthopaedic biomaterials are to be considered mainly to restore the function and mobility of the native tissue which is to be replaced. The materials which are generally used for orthopaedic application are ceramics, polymers, and metals. Various ceramic materials in different combination of alumina, zirconia, spinel, hydroxyapatite and bioglass are used for musculoskeletal restoration as some are bio-inert, bioresorable, and bioactive [1]. Similarly, polymers like polymethyl methacrylate PMMA and ultrahigh-molecular-weight polyethylene (UHMWPE) are used for cyclic load-bearing conditions in the knee and hip arthroplasty [2]. In spite of a large number of advantages, ceramic materials possess poor mechanical properties such as fracture toughness and bending strength due to their brittleness. Therefore, prostheses of pure ceramics are generally not preferred for load-bearing applications [3, 4]. The use of polymers is limited to the repair of small bone fractures and soft tissues due to their low strength [4] and their inability to sustain mechanical forces present in joint replacement surgery. The problems associated with ceramics and polymers were mitigated by the use of metals and alloys.

Various metals and their alloys like Stainless steel, Co-Cr-Mo alloys, Magnesium, Ti and Ti alloys are being used for orthopaedic application [5, 6, 7]. Among these metallic materials, Ti and its alloy possess all the characteristics of an ideal implant such as excellent

mechanical properties, corrosion resistance and good biocompatibility. But the main reason for failure of Ti-based implants can be attributed to the "Stress Shielding" effect which is being caused due to the difference in strength and elastic modulus of Ti with respect to that of host bone. Young's modulus of natural bone varies between 10 to 30 GPa which is too less when compared with respect to Titanium and its alloy (55-110 GPa) [4]. This mismatch in mechanical property leads to non-uniform loading resulting in bone resorption and eventually failure of the implant [6, 8, 9]. Hence, in order to prevent premature implant failure, various types of efforts have been made for the reduction of stress shielding effect. The development of porous Ti implant by incorporation of pores into the Ti matrix is one of the common approaches now a day [10]. The presence of pores decreases Young's modulus of the Ti-based implant and brings it closer to that of natural bone, resulting in the reduction of stress shielding effect. Also, the presence of pores provides an interconnected porous framework, which helps in growth of new tissues. Pores also help in excellent mechanical interlocking and biological fixation between Ti implant and the host bone, which results in a homogeneous stress transfer between bone and implant and consequent bone in-growth [11]. It has been reported that porous materials with a large pore size in the range of 200-500μm and small pores in the range of few micrometres can be used as a human bone substitute as they are favourable for growth of bone tissue and humoral transmission [12, 13, 14]. Therefore, a porous Ti scaffold with controlled porosity and microstructure can be a promising implant material for orthopaedic application.

Although, porous Ti implant improves stress shielding effect, but the presence of pores also reduces the strength of the implant simultaneously. One of the common approaches to increase the strength of the porous Ti scaffold is the use of ceramic particle

reinforcements in Ti matrix [15, 16]. Han et al. [17] reported that there is an improvement in strength of porous Ti material using SiO_2 ceramic particles as a reinforcement agent. They used nano biocompatible SiO_2 particles as reinforcement in Ti matrix to fabricate Ti-SiO_2 composite which improved both biocompatibility and strength of the scaffold. Also, reports suggested that Ti alloy coated with a SiO_2 layer can significantly improve the biocompatibility, bioactivity and corrosion resistance [18]. The use of SiO_2 particles as ceramic reinforcement has been preferred due to its biocompatibility, bioactivity, corrosion resistance, and antioxidant capacity. Thus, considering the importance of porous Ti scaffolds in orthopaedic application along with the advantages of use of ceramic particles as reinforcement in the Ti matrix, the present research work attempts to design and develop porous Ti-SiO_2 composite scaffold suitable for orthopaedic application. Mercury intrusion porosimetry (MIP) is a method used to measure the porosity of a material. The literature suggested that the sucrose as fugitive material for processing and fabrication of porous Ti scaffold [19]. Thus, the present work is a strong motivation for use of rice husk (RH) powder as natural fugitive material along with sucrose which also acted as another fugitive material for processing and fabrication of porous Ti implant.

The idea behind the use of RH was to incorporate silica and pores in Ti matrix and sucrose was to act as a binder and pore former. Thus, RH and sucrose collectively created pores after burnout during processing. It may be mentioned here that the combined use of RH and sucrose can be used as fugitive in fabrication of porous ceramics [20, 21, 22], but its use to fabricate porous Ti-SiO_2 composite has not been reported earlier. Considering the unique advantages of combined use of RH and sucrose to incorporate both SiO_2 and pores, the present work was aimed to develop a porous Ti-SiO_2 composite using powder metallurgy

technique. Various other advantages of the use of RH and sucrose as space holder materials are low decomposition temperature with simple processing, chemical inertness with Ti matrix, low cost and eco-friendly. In the presented work, an effort was made to develop porous Ti-SiO_2 composites with a wide range of tailored microstructures by proper control of composition and processing parameters. The developed composite was characterized physically, mechanically and biologically and a comparative study was made with the properties of natural bone based on literature reports.

5.2.Experimental Procedure

5.2.1. Processing and Characterization of Rice Husk (RH)

RH was collected from local rice mill and was thoroughly cleaned for complete removal of impurities such as sand, clay, dust, etc with distilled water. Then clean RH was first dried in the open atmosphere for 2 hours followed by oven drying at 150°C for 24 hours [20]. Grinding machine (Kenstar Prince Royal, Videocon Industries Limited India) was used to convert the rice husk (RH) into rice husk powder. The obtained RH powder was sieved in a sieve shaker (J.S Industries Limited) to collect the RH powder of three different mesh sizes i.e. <180 μm, 180-355 μm and 355-600 μm (British Standard Specification). Degradation behaviour of RH under the influence of temperature was analysed using Thermogravimetric analysis (Simultaneous Thermal Analysers, Model Labsus, Setaram, France). The samples were heated at a rate of 1°C/min up to 600°C. X-ray diffraction was carried out to analyse the phases present in RH powder after burning at 480°C for 2 hours [23]. The standard flow chart of the whole experimental process is shown in **Fig. 5.1**.

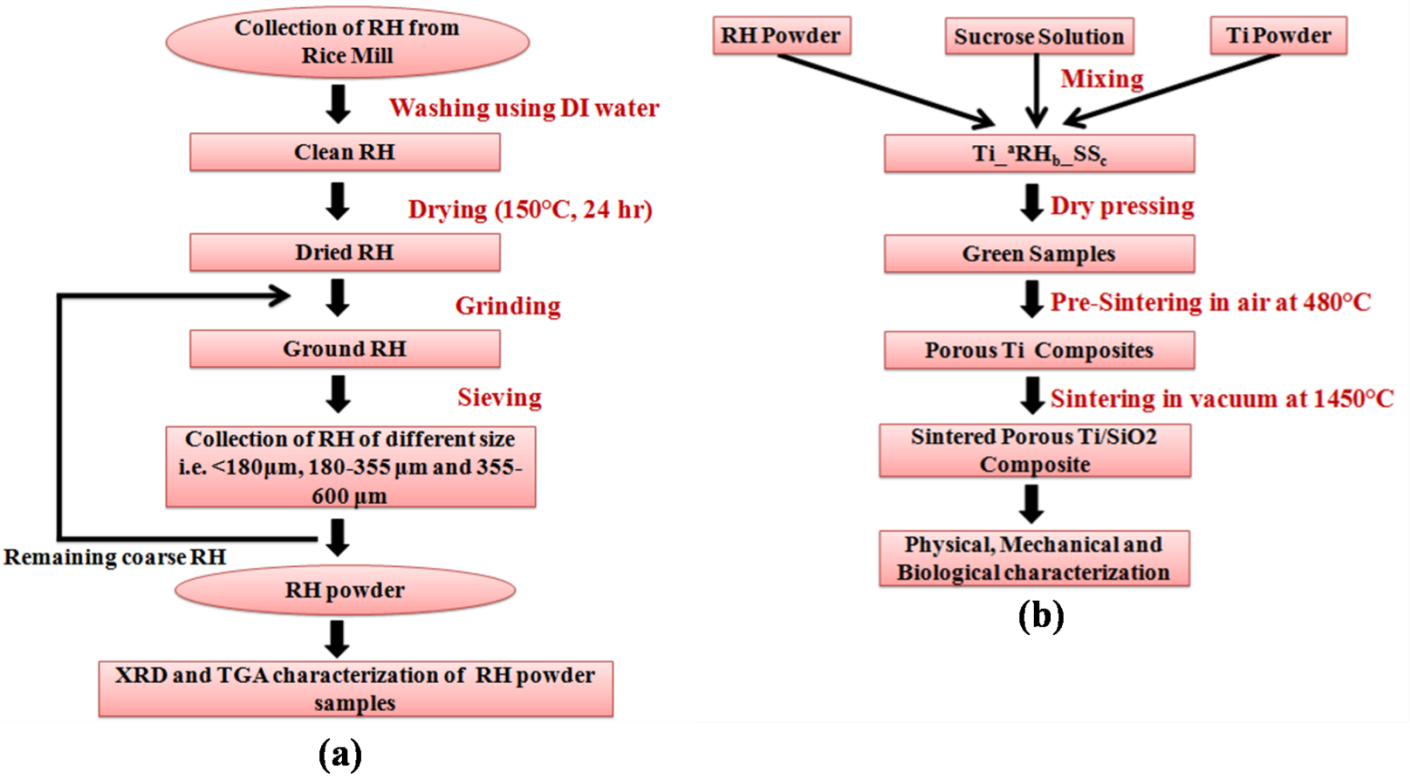

Fig.5.1 Standard process flow chart of (a) Processing of RH powder and (b) Fabrication of Porous Ti-SiO_2 scaffold

5.2.2. Composition Formulation and Sample Preparation

Ti powder (149µm, 98.5% pure, CDH (P) Ltd. India) was used for sample preparation. RH powder of average particle sizes below 180 µm, 180-355µm and 355-600 µm was used as space holder fugitive material. Sucrose (Merck Specialties Pvt. Limited, Mumbai, India) in the form of solution was used as binder which also acted as a pore former. Different mixture compositions were prepared in a mortar and pestle using Ti powder with 5, 10, 15 and 20wt% RH powder separately. For each mixture, 0.04wt% sucrose solution was added as a binder for making green pellets. All sample compositions are expressed with a general formula Ti_$^{a}RH_b$_SS_c where Ti represents Titanium powder; RH represents rice husk powder and SS represents sucrose solution. In the above formula a, b, and c are the variables where

'a' represents the size of RH powder in μm, 'b' represents wt% of RH powder and 'c' represents wt% of sucrose solution. Green samples were prepared through dry pressing using circular disk-shaped steel die of 16 mm diameter in a hydraulic press. The schematic representation of sample preparation is shown in **Fig. 5.1 (b)**. After conducting series of experiments for finding suitable composition, twelve compositions resulted in green compacts without any visible defect. The list of all feasible compositions is given in **Table 5.1**. Representative Green samples are shown in **Fig. 5.2**. The green compact was dried in an oven at 150°C for 24 hours. Then, the dried sample was heat-treated at 480°C in ambient atmospheric furnace at 3°C/min for removal of space holder through fugitive burnout and formation of pore. Finally, sintering of the porous Ti samples was carried out in a vacuum furnace at 1450°C.

Table 5.1 List of feasible compositions (wt% basis) which are fabricated successfully into porous Ti-SiO_2 composite.

RH size (μm)	**RH (wt. %)**			
	5	**10**	**15**	**20**
<180	$Ti\_^{<180}RH_5\_SS_{0.04}$ **(T_1)**	$Ti\_^{<180}RH_{10}\_SS_{0.04}$ **(T_4)**	$Ti\_^{<180}RH_{15}\_SS_{0.04}$ **(T_7)**	$Ti\_^{<180}RH_{20}\_SS_{0.04}$ **(T_{10})**
180-355	$Ti\_^{180-355}RH_5\_SS_{0.04}$ **(T_2)**	$Ti\_^{180-355}RH_{10}\_SS_{0.04}$ **(T_5)**	$Ti\_^{180-355}RH_{15}\_SS_{0.04}$ **(T_8)**	$Ti\_^{180-355}RH_{20}\_SS_{0.04}$ **(T_{11})**
355-600	$Ti\_^{355-600}RH_5\_SS_{0.04}$ **(T_3)**	$Ti\_^{355-600}RH_{10}\_SS_{0.04}$ **(T_6)**	$Ti\_^{355-600}RH_{15}\_SS_{0.04}$ **(T_9)**	$Ti\_^{355-600}RH_{20}\_SS_{0.04}$ **(T_{12})**

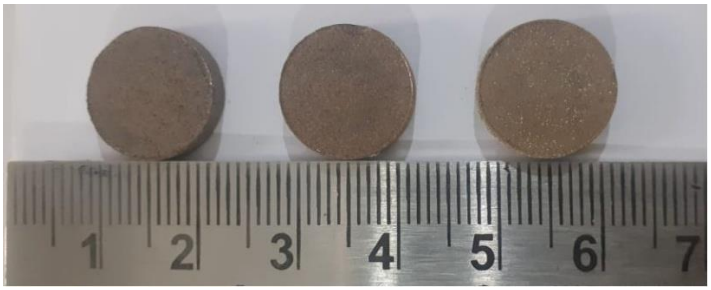

Fig.5.2 Representative Green samples prepared using Ti powder, RH and sucrose

5.2.3. Physical and mechanical behaviour of composite samples

Sintered porous samples were characterized for apparent porosity using water immersion method based on the Archimedes principle. The porosity of the developed scaffold was measured using Archimedes principle in the present work, however there are different advanced techniques to measure porosity like mercury intrusion porosimetry (MIP) and Brunauer-Emmett-Teller (BET) surface area analysis for porosity measurement and quantification of active surface area. In MIP, a sample is first saturated with a liquid, typically mercury, and then pressurized with the mercury. As the pressure increases, the mercury is forced into the smaller pores of the material. By measuring the pressure at which the mercury begins to intrude into the sample, and the pressure at which it fills all of the pores, the porosity of the sample can be calculated. The sample is also examined under a microscope to determine the size and distribution of the pores. The sample must be in a solid form, and should be homogeneous and free of cracks, voids, and other defects. The sample should also be cleaned and dried thoroughly before testing. Similarly, The Brunauer-Emmett-Teller (BET) method is a widely used technique for determining the specific surface area of a material. The BET method is based on the principle that the amount of adsorbed gas on a solid material is directly proportional to the surface area of the material. In the BET method,

a sample is first evacuated and then exposed to a gas, typically nitrogen, at a specific pressure and temperature. As the gas adsorbs onto the surface of the material, the amount of adsorbed gas is measured as a function of pressure. This data is then used to determine the surface area of the material using a mathematical equation known as the BET equation. a study on Ti6Al4V samples produced by powder metallurgy found that the specific surface area was in the range of 0.1-0.2 m^2/g. Another study on Ti6Al4V samples produced by selective laser melting found that the specific surface area was as low as 0.03 m^2/g. A study on Ti6Al4V samples produced by casting found that the specific surface area was as high as 0.15 m^2/g. Since the samples in the present case consist of cracks, voids and inhomogeneous therefore these characterizations were not preferred. The theoretical density of pure Ti was taken as 4.51 gm/cc for evaluation of porosity. The microstructure and surface morphology of sintered porous samples were characterized using Scanning Electron Microscopy (FEI Inspect S30 Sweden). Phase analysis of the sintered samples was carried out using an X-ray diffractometer (Miniflex II, Desktop X-Ray Diffractor, Rigaku Corporation, Japan) with CuK_α radiation (wavelength 1.542Å). Elemental analysis of the samples was studied using Energy Dispersive Spectroscopy (EDS). The compressive strength of the samples was measured in a UTM machine (Shimadzu Corporation, Japan) and the elastic modulus was evaluated directly from the slope of elastic part of the stress-strain curve.

5.2.4. Biofilm Formation

Biofilm formation was evaluated as per the procedure reported in the literature [26]. Staphylococcus aureus (S. aureus) strain (ATCC 29213) was used for biofilm formation. The porous composite samples were sterilized using HNO_3 followed by autoclaving. The overnight culture of S.aureus was used as inoculum to make a fresh culture. The sterile

samples were placed in sterile flat-bottom jars containing sterile tryptone soya bath (TSB). In this experiment, fresh culture of 10^5cells/ml of S.aureus was added and it was incubated at 37°C for 24 hours. Planktonic bacteria were removed from the samples by rinsing it with sterile phosphate buffer saline (PBS). The biofilm was fixed using 4% paraformaldehyde at 4°C in PBS for 2 hours and then dehydrated in increasing concentration of ethanol (50%, 70%, 90% and100%). The samples were finally dried, mounted and then sputter-coated with carbon. The samples were analysed under SEM to observe the biofilm formation. The biofilm formation was quantified using crystal violet assay. In this assay, biofilm was grown on the porous composite samples using the above-described procedure. Planktonic bacteria were removed from the samples by rinsing it with sterile PBS. The remaining attached bacteria were fixed using 100% ethanol and stained with 0.41% crystal violet in 12% ethanol. Further, the samples were washed with sterile distilled water and kept overnight for drying. The crystal violet was then eluted using 100% ethanol. A 200 µl of an aliquot from each sample was transferred to a well in 96 well plates and the absorbance was measured at 600 nm.

5.2.5. Cell Culture Study

The cell culture study on the prepared samples as discussed previously was observed to check its bio function. For this purpose, MTT assay osteoblast-like MC3T3-E1 cell line sub-clone 4 (ATCC) were taken.

5.2.5.1. MTT Assay

To check the biocompatibility of the composites, MTT (3-(4,5-dimethyl thiazol-2-yl)-2,5-diphenyl tetrazolium bromide) was performed. The MTT assay measures the mitochondrial

activity of the cells, which reflects the viable cell number. Sterile Ti-SiO_2composites were initially incubated with 1ml sterile cell culture media in 12 well plates. Further, osteoblasts cell line MC3T3-E1 sub-clone 4were seeded at a density of 1×10^5 cells per well and growth media was added. The plates were incubated at 37°C in a CO_2 incubator for 7days. On the 7^{th} day, the media was discarded and 1ml of MTT reagent was added to each well. After 3 hours of incubation, the media plus MTT reagent were discarded. The formazan reaction product was dissolved in 1ml DMSO. OD at 570 nm was measured after 15 minutes of incubation in shaker conditions. Cells without composites and only DMSO were used as control and blank simultaneously.

5.2.6. Evaluation of Bioactivity

The bioactivity of the samples was examined by using simulated body fluid (SBF) also. Since ionic concentration of the SBF is similar to that of human blood plasma. Therefore, it can stimulate the properties of human plasma when the samples are immersed in it for fixed interval of time.SBF was prepared in the laboratory according to the Kokubo method [24]. The SBF mixing order and amount of reagents mixed in 1000ml deionized water are given in **Table 5.2**. Fabricated samples were immersed in an aqueous SBF solution for 7 and 14 days. After the 7^{th} and 14^{th} day, the samples were removed from the SBF and dried in a vacuum oven for removal of the absorbed moisture. Scanning electron microscopy with EDS of dried samples was performed to observe the formation of apatite on the surface of samples [25].

Table 5.2 Chemical compositions of SBF and their order of mixing.

Order Number	Reagents	Amount(g) in 1000 ml of deionized water
1	NaCl	8.035
2	$NaHCO_3$	0.355
3	KCl	0.225
4	$K_2HPO_4.3H_2O$	0.231
5	$MgCl_2.6H_2O$	0.311
6	1.0 M HCl	39.0
7	$CaCl_2$	0.292
8	Na_2SO_4	0.072
9	$(HOCH_2)CNH_2$	6.118
10	1.0 M HCl	Till pH value reaches 7.4

5.3. Results and Discussion

5.3.1. Thermal Analysis of RH and Sucrose

Thermogravimetric analysis data of RH and sucrose is shown in **Fig. 5.3**. The graph shows that the thermal decomposition behaviour of both RH and sucrose in air is similar in nature. Very slow weight loss behaviour was observed up to approximately 200°C followed by a sharp decrease in the temperature range of 200°C-480°C, indicating major weight loss. Beyond this temperature, the weight loss is almost negligible for both RH and sucrose. The weight loss of the RH and sucrose under the influence of temperature in ambient atmosphere can be attributed to following steps like drying (40°C-150°C) for moisture removal, burnout of organic content (215°C-350°C) and then degradation of carbonaceous phases like

cellulose and hemicelluloses (at temperature greater than 350°C) [26]. Similarly, Thermal decomposition behaviour of sucrose was analysed by heating it in ambient atmosphere between 180°C to 480°C [27]. The analysed decomposition behaviour of RH and sucrose was utilised for complete fugitive removal from green samples to get defect-free samples. A single fugitive burnout schedule was maintained for all samples in the present research study.

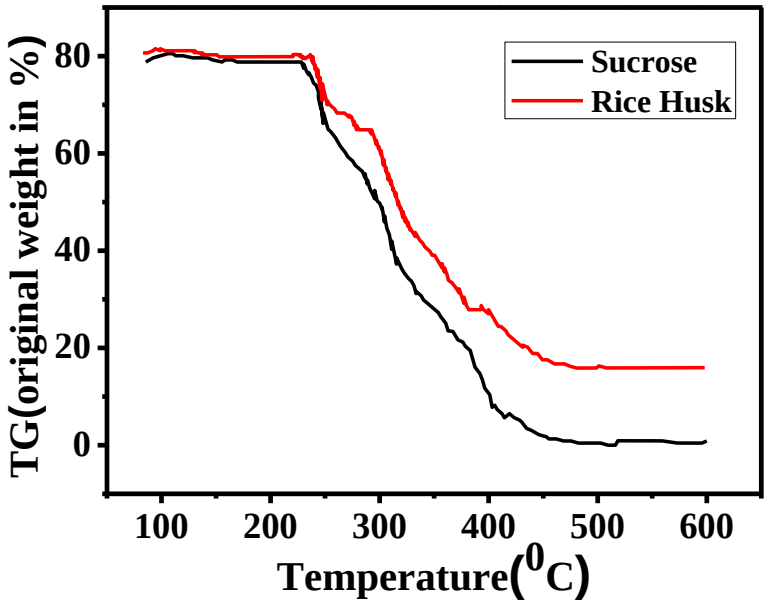

Fig.5.3 TG analysis of RH powder and sucrose in air

Fig.5.3 shows that the ash content of sucrose is negligible and in case of rice husk, nearly15% ash is obtained as a result of thermal degradation of RH. The amount of rice husk ash, obtained is within range of 13-29% as reported in literature [28]. According to Matori et al. [23], rice husk ash contains silica as main constituent in the range of 92-97%. X-ray diffraction patterns of rice husk heat treated at 480°C and 1450°C are shown in **Fig.5.4** and **Fig.5.5** respectively. XRD pattern of the rice husk ash, heat treated at 1450°C, were analysed

and it was found that a peak at d=4.06Å corresponds to α-crystobalite, which was a crystalline phase of silica. A similar observation had been also reported by other researchers [29]. It is important to mention that silica present in burnout residue was helpful in the present study as SiO_2 can be incorporated in the Ti matrix during heat treatment to form Ti-SiO_2 green compacts.

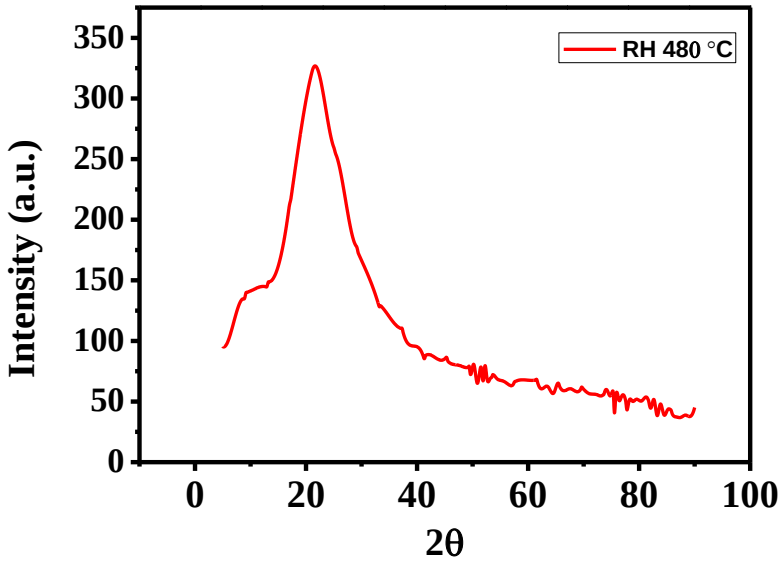

Fig.5.4 X-ray diffraction pattern of residue (RHA) left after heat treatment of RH powder at 480°C

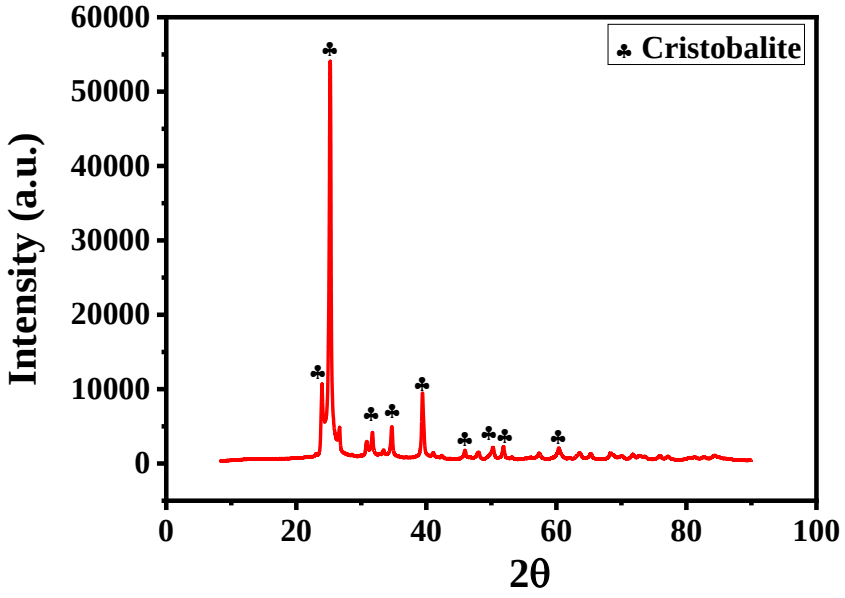

Fig.5.5 X-ray diffraction pattern of residue (RHA) left after heat treatment of RH powder at 1450°C

5.3.2. Processing and fabrication of porous Ti-SiO_2 composite

The fabrication of porous Ti-SiO_2 composite samples were started with the processing of rice husk, which included cleaning, drying, size reduction and then their separation through sieving in order to get RH powder. For size reduction of RH, the first step involved in the experiment was to determine the grinding ability of RH. Accordingly, drying of RH at 150°C for for 24 hours was preferred out of a few initial trials to get maximum possible output through grinding. Then, homogeneous mixing of dense Ti powder (4.5gm/cc) and lightweight RH powder (0.86-1.14 g/cc) in various size ranges, according to selected composition, was necessary to optimize. The addition of sucrose binder in the form of solution helped in homogeneous and uniform mixing of Ti-RH mixture. 0.04 wt% sucrose solutions (60 wt% concentration) were used as a binder for the preparation of samples of all

compositions as mentioned in Table 1. Sucrose solution was used for multiple purposes like providing sufficient strength to the green sample with homogeneous mixing of Ti powder and RH powder before compaction. All samples as mentioned in **Table 5.1** contained a fixed quantity of sucrose in their composition. The amount of sucrose was optimized to have maximum possible green strength with minimum defects. The use of sucrose as a binder for making green ceramic samples was also reported by Schilling et al. [30]. All samples fabricated with composition as mentioned in **Table 5.1**, were free from defects and they have sufficient green strength. They were handled properly for further processing stages without any shape variation. It is significant to mention that compositions with more than 20 wt% of RH cannot be shaped into green pellets of required dimensional accuracy even after using maximum possible quantity of binder. Excess amount of binder in the composition results in sticking and squeezing out of sample powder from the mould surface during compaction. Hence, processing of porous Ti samples with compositions other than those mentioned in **Table 5.1**, were not feasible using RH pore former in the specified size range.

Green samples in the form of cylindrical pellets, prepared through dry pressing in the present study, were free from any visible defects and have good surface finish. Representations of green samples are shown in **Fig.5.2**. The drying shrinkage of green samples was almost negligible and the green density varied from 2.3 to 3.2 g/cc (51.11% to 71.11% TD). Green samples were heat-treated at 480°C for removal of space holder material as already discussed in experimental procedure. After the removal of space holder, the samples were defect-free. All samples after pre-sintering were sintered at 1450°C in vacuum to get porous Ti-SiO_2 scaffold. The sintered samples were free from any visible defects and their linear firing shrinkage value is in the range of 7 to 9%.

5.3.3. Phase analysis of Ti-SiO_2 composite scaffold

Fig. 5.6 shows the XRD patterns of the developed porous Ti-SiO_2 composites. The intense peak corresponds to Ti in all samples. Since, the amount of silica derived from RH is too less therefore the peaks of SiO_2 and $TiSi_2$ were hard to be observed in the diffraction pattern along with Ti peak in the range of 35°-40°. However, the energy dispersive spectroscopy observation discussed in section 5.3.4 confirms the introduction of silica in Ti matrix during heat treatment of Ti_$^{a}RH_b$_SS_c samples. The silica presented in Ti matrix was the result of residue of RH after burning. It is worth to mention that the amount of silica present in Ti-SiO_2 composite is directly proportional to the amount of RH in the sample. Wang et.al. [33] reported the presence of $TiSi_2$ phase which may be due to the reaction between Ti and SiO_2 during high-temperature sintering. XRD pattern of the remaing samples shows no major difference in the phases present in <180 µm and 355-600 µm samples so, graphical illustration of these compositions are not included.

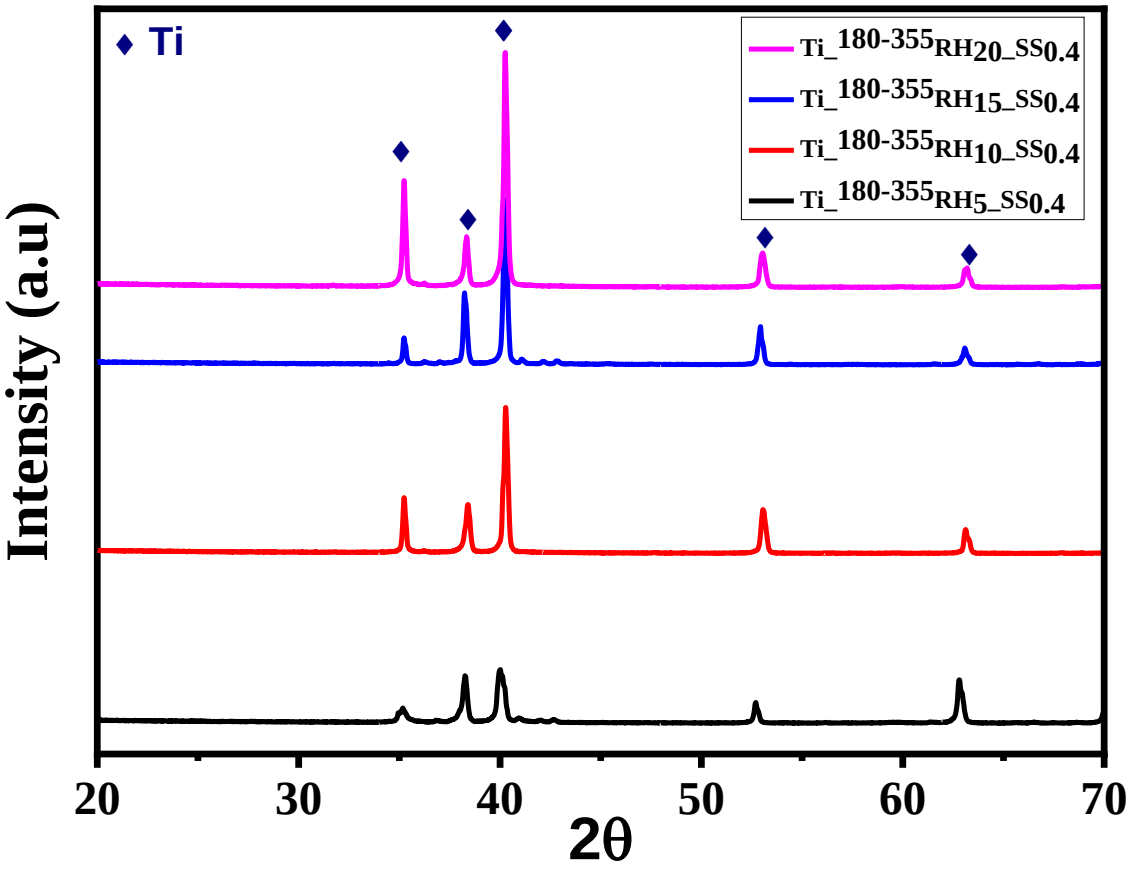

Fig. 5.6. XRD pattern of porous Ti-SiO_2 composites with different RH content sintered at 1450°C

5.3.4. Porosity and Microstructure

Fig. 5.7 (a) shows the variation of open porosity with wt% of RH for different particle sizes of RH powder. It was observed that the open porosity of samples increased linearly with increase in RH content from 5 to 20 wt% irrespective of the particle size of RH powder as shown in **Fig. 5.7 (a)**. A lowest porosity about 15% and a maximum porosity of 34%were obtained in the samples with compositions T_1 and T_{12} respectively. It can also be noted that

the porosity of samples, prepared with larger size RH space holder, was always higher as compared to those prepared using finer size RH powder and also irrespective of the wt% addition in the Ti matrix. The porosity in the samples was created by incorporation of pores into the Ti matrix as a result of burnout of RH and sucrose. Similar observation was also confirmed from the SEM micrographs. **Fig. 5.8 (a-f)** shows the surface morphology of the scaffold under larger magnification. Rough surface can be observed in the micrograph which is due to carbonization of randomly distributed RH powder. EDS profile of each scaffold is shown along with their corresponding SEM images. EDS profile confirms that the pores formed by space holder material contain silica (Si). **Fig. 5.8 (a-c)** shows SEM micrographs of porous Ti-SiO_2 scaffold with 10% RH of different sizes i.e., <180 μm, 180-355 μm and 355-600 μm respectively. It was observed that increase in size of RH powders, the porosity of the scaffold was also increasing. Similarly, **Fig. 5.8 (d-f)** shows SEM micrographs of porous Ti-SiO_2 scaffold with 20% RH of different sizes i.e., <180 μm, 180-355 μm and 355-600 μm respectively. Due to increase in size of RH, the porosity of the scaffold was also increasing. Furthermore, it can be observed from the SEM image that the amount of RH in the composition increased the pore interconnectivity. This can be explained by the fact that as the amount of RH powder in Ti matrix increased, the number of large individual RH particles in the matrix connected to each other among the pores and make them open. The SEM micrographs as shown in **Fig. 5.8** shows that the volume fraction of porosity increases with increase in RH content. The formation of pores inside the pellets, confirmed that all the pore formers were converted into pores after heat treatment and pore volume and volume of RH particles were proportional to each other. These results suggested that by varying the amount and size of RH space holder, the porosity and pore microstructure of the samples can be

tailored. Several reports suggested that the porous Ti scaffolds with porosity in the range of 5-58% are suitable for implant application [19, 31-34]. Fig. 5.9 shows SEM micrograph of porous Ti-SiO_2 composites fabricated using 5 wt% (a-c) and 15 wt% (d-f) RH powder of sizes < 180 µm, 180-355µm, and 355-600 µm respectively.

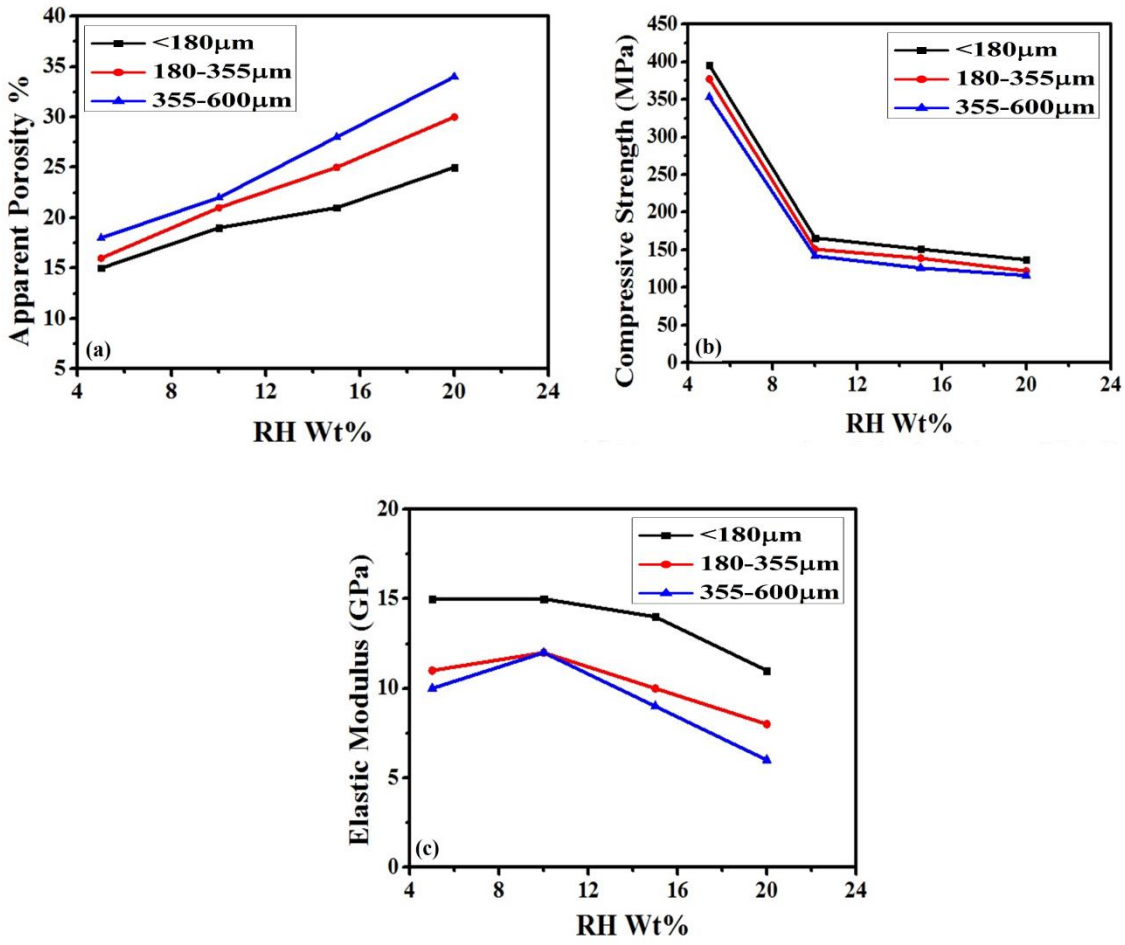

Fig. 5.7. Effect of RH content and RH size on (a) apparent porosity, (b) compressive strength and (c) elastic modulus of porous Ti-SiO_2composites

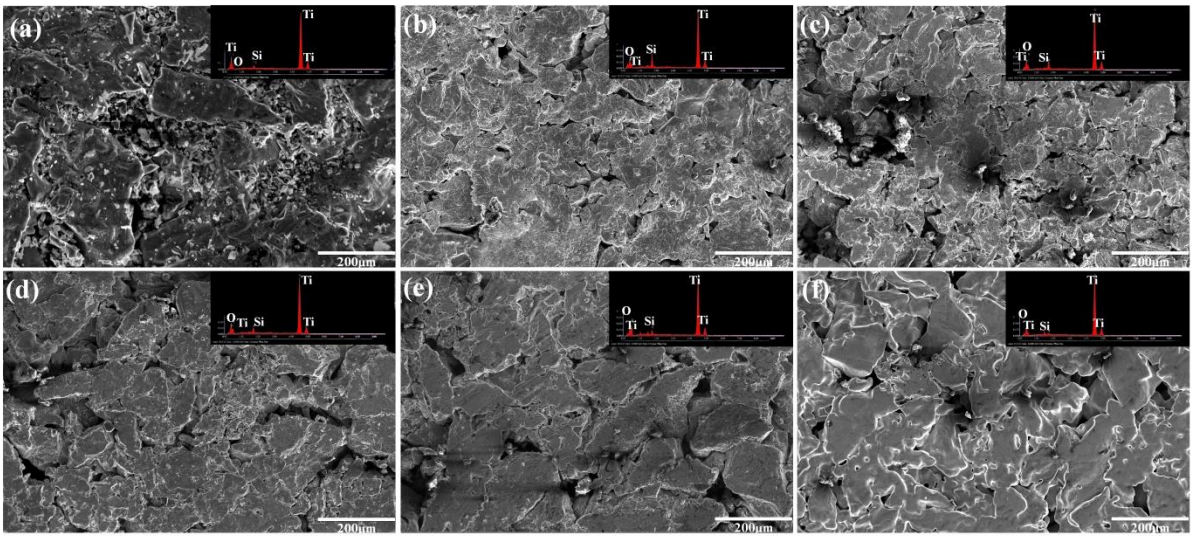

Fig. 5.8. SEM micrograph of porous Ti-SiO_2 composites fabricated using 10 wt% (a-c) and 20 wt% (d-f) RH powder of sizes < 180 µm, 180-355µm, and 355-600 µm respectively

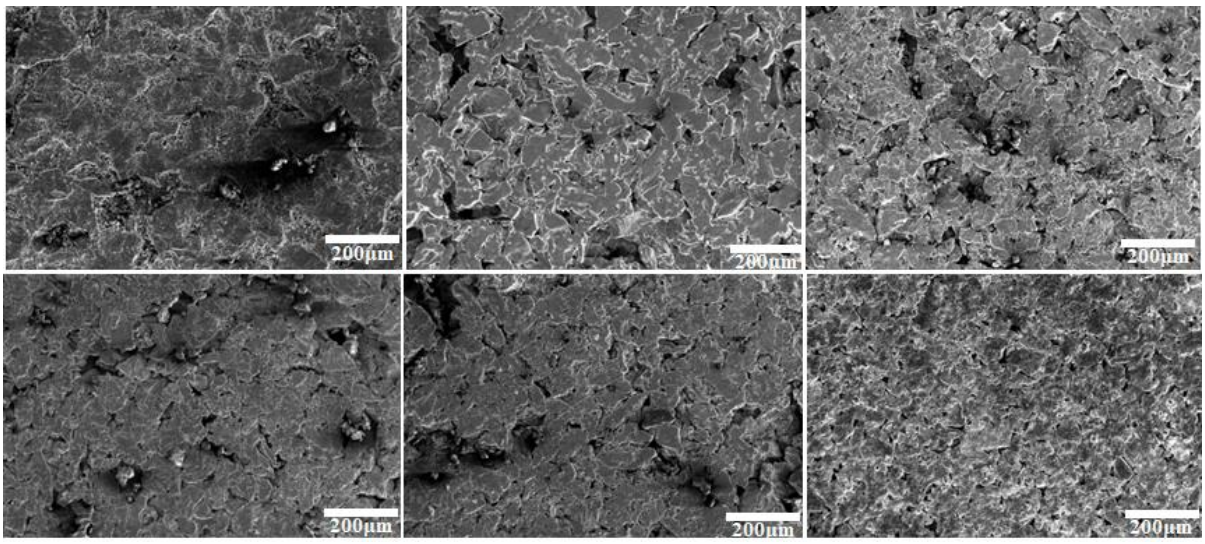

Fig. 5.9. SEM micrograph of porous Ti-SiO_2 composites fabricated using 5 wt% (a-c) and 15 wt% (d-f) RH powder of sizes < 180 µm, 180-355µm, and 355-600 µm respectively

5.3.5. Mechanical Properties

Fig. 5.7 (b) shows the variation of compressive strength of porous Ti-SiO_2 samples with wt% of RH and different sizes of RH powder. It was observed that the compressive strength of samples decreased linearly with increase in RH content from 5 to 20wt% for each size of RH powder. Ti-SiO_2 composites having 20wt% RH showed more porosity compared to those having 5wt% RH, irrespective of the size of RH powder. It was due to the fact that preheated samples, prepared with 20wt% RH provided more space during fugitive burnout. Similarly, compressive strength was better for composites, prepared using 5wt% RH due to comparatively lesser porosity. Also, the strength of samples prepared with finer size RH powder, was always higher for a fixed amount of RH addition in the composition. Porous Ti-SiO_2 composites with compressive strength in the range of 116 to 396 MPa, having porosity 15-34%, was obtained in the present study. It can be concluded that as the volume fraction and size of RH increased in the composition, the compressive strength of samples decreased. It was due to the fact that porosity and mechanical properties are inversely proportional. Sample with T_1 composition, exhibited lowest porosity, results in maximum compressive strength. Similarly, samples with T_{12} composition corresponding to highest porosity, showed minimum compressive strength. The elastic modulus of the developed porous Ti-SiO_2 composite samples was directly estimated from the slope of the elastic part of the stress-strain curve. **Fig. 5.7 (c)** shows the variation of elastic modulus of samples, prepared with increased wt% of RH for different sizes of RH powder. It was observed that the value of elastic modulus decreased linearly as the apparent porosity of samples increased. Porous scaffolds with 15% and 34%apparent porosity possessed elastic modulus value 15 GPa and 6 GPa respectively. Thus, it can be concluded that the Elastic modulus of the Ti compacts can

be tailored in the range of 6-15 GPa by introducing pore in Ti matrix with the help of RH as a space holder material. The obtained properties of Ti-SiO_2 composite scaffolds like porosity, compressive strength and elastic modulus were compared with properties of natural bone and also of properties, obtained in previously reported work as shown in **Table 5.3**. It was found that the measured properties of the scaffold are in the range of previously reported work.

Table 5.3 Property comparison of porous Ti-SiO_2composite with previously reported work and with human cortical bone

Space Holder Material/ Processing Method/ Natural Bone	**Porosity (%)**	**Young's Modulus (GPa)**	**Compressive Strength (MPa)**	**Ref.**
RH	15-34	6-15	116-396	Present work
Sucrose	20-54	12-18.5	NA	[19]
Plasma rotating electrode process (PERP) and Gas Atomization process	5-37	NA	5-300	[31]
Laser Engineered net shaping (LENS^{TM}) process	17-58	2.6-44	NA	[32]
RH	24-35.5	NA	440-938	[33]
Molybdenum Wire	32-47	26-62	76-192	[34]
Human Cortical Bone	5-10	3-30	80-120	[35, 36]

5.3.6. Evaluation of Bioactivity

In vitro bioactivity of the developed porous Ti-SiO_2 composites (Ti_ $^{<180}RH_{20}$_$SS_{0.04}$) was evaluated by immersing the samples in SBF solution for different time periods i.e. 7 days and 14 days. **Fig. 5.10 (a, b)** shows the SEM micrographs of porous Ti-SiO_2 scaffolds soaked in SBF for 7 and 14 days respectively. In contrast to the sample surface before immersion,the deposition of a new bone-like apatite having spherical shape was observed on the surface of

samples after immersion in SBF. The EDS report suggested that the surface deposits on the samples are a kind of apatite (calcium phosphate). It was also observed that the concentration of Ca and P ions in the deposits increased with increasing the incubation period of samples from 7 days to 14 days. **Fig. 5.11 (a-c)** shows schematic way to represent the processing of formation of the layer of apatite on the surface of Ti-SiO_2 composite scaffold for time of immersion in SBF solution of 1^{st}, 7^{th} and 14^{th} day respectively. The schematic diagram shows the formation of apatite nuclei on the surface of the scaffold after the 7th day of immersion in SBF solution, this is due to the fact that Ti forms a passive oxide film when exposed to ambient. During the alkali treatment process, this oxide film reacts with OH^- ions present in SBF solution and forms a Ti-OH layer throughout the surface. Further, the Ti-OH layer combines with Ca^{2+} ion and forms calcium titanate. This calcium titanate combines with negatively charged phosphate ion and results in the formation of calcium phosphate nuclei. As the soaking time increases (from 7^{th} day to 14^{th} day) this nuclei continues to grow throughout the surface by consuming calcium and phosphate ions present in SBF solution [37]. In addition to this, the presence of Ti and Si ions were also detected in EDS analysis of the scaffold, corresponding to the Ti matrix and SiO_2 incorporated from RH. Results obtained from the mechanical property and biological behaviour of porous Ti-SO_2 scaffolds showed a nature, which was similar to that of human cortical bone. Hence it can be predicted that the porous Ti-SiO_2 composites scaffolds are suitable for implant applications.

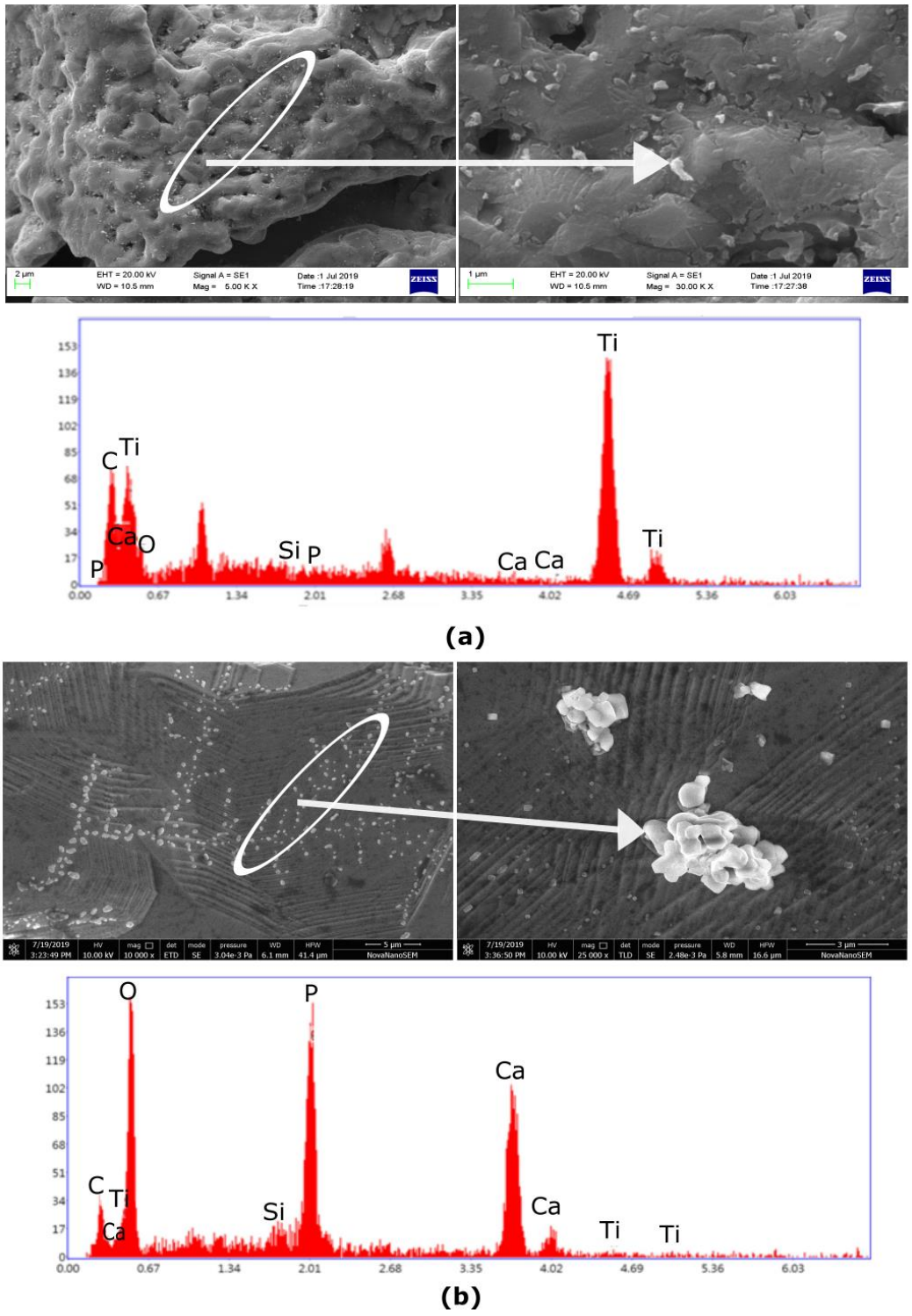

Fig. 5.10. SEM and EDS micrograph of Ti_ $^{<180}RH_{20}$_$SS_{0.04}$ scaffold after dipping in SBF for (a) 7 days and (b) 14 days

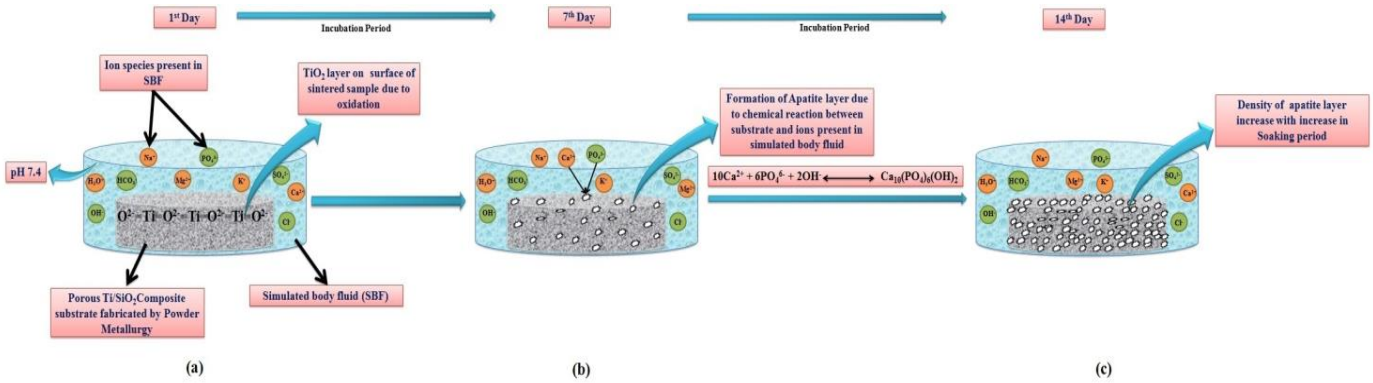

Fig. 5.11. Schematic diagram showing the mechanism of formation of apatite layer on the surface Ti-SiO_2 scaffold when soaked in SBF solution on (a) 1st day, (b) 7th day and, (c) 14th day

5.3.7. Biofilm Formation

Fig. 5.12 shows the result of biofilm quantification i.e., the amount of biofilm formed on different porous Ti-SiO_2 scaffold, estimated using crystal violet assay. It can be observed that in comparison to pure Ti sample, the other samples showed higher absorbance, indicating higher bacterial adherence. The higher value of bacterial adherence can be attributed due to the presence of porosity in the developed samples. Due to higher porosity, the surface roughness of the scaffold was increased which caused higher bacterial adherence. Similar observation regarding the bacterial adhesion influenced by surface topography has been reported in literatures [34, 35, 36]. The above conclusion was also supported by SEM images as shown in **Fig. 5.13**. It showed the trend of bacterial adherence, according to which absorbance was increased with the increase in the percentage of RH. A more detail observation of the trend of biofilm formation behaviour showed that among all the composition displayed, the composition T_{10} ($Ti\_^{<180}RH_{20}\_SS_{0.04}$) showed least biofilm formation just indicating more suitability for orthopaedic applications. The reason behind the

formation of lesser biofilm can be attributed to maximum amount (20 wt%) and smaller size of RH (<180 μm) of RH added in the mentioned sample. The mentioned amount of RH will produce relatively large amount of silica with small pore size in the Ti matrix. It is well known that silica particles are effective at killing biofilm-based microbes thus, T_{10} shows least biofilm formation. Also it is reported that the scaffold with minimum biofilm formed are much better for orthopaedic application in comparison to those having more biofilm formation. The reason for this is that biofilm can produce the risk of microorganism to increase ineffectivess with antibiotics. This can give further the complication to human health, increasing inflammation and other health issues [38, 39].

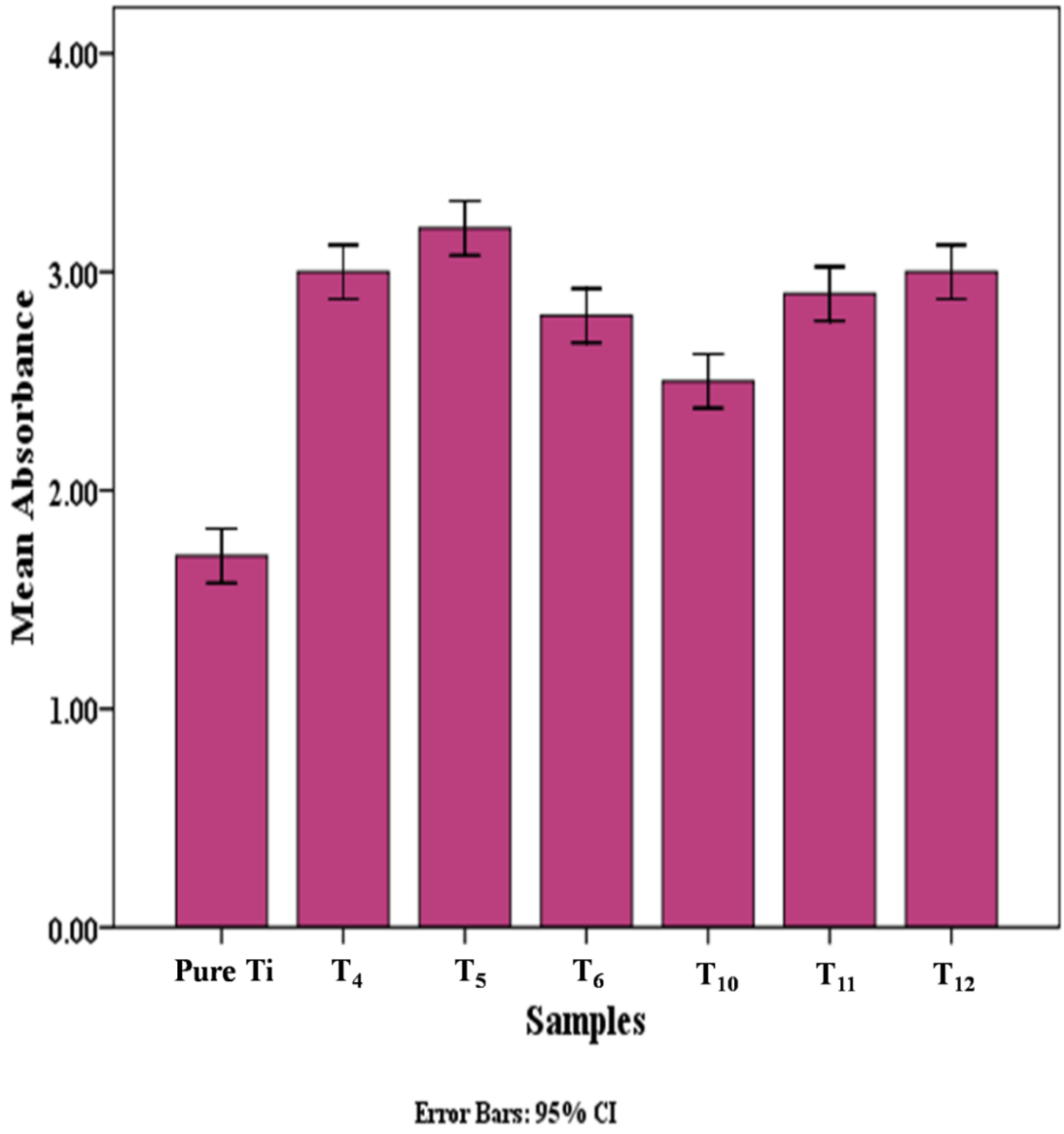

Fig. 5.12. Biofilm quantification: The amount of biofilm formed on different composites was estimated using a crystal violet assay.

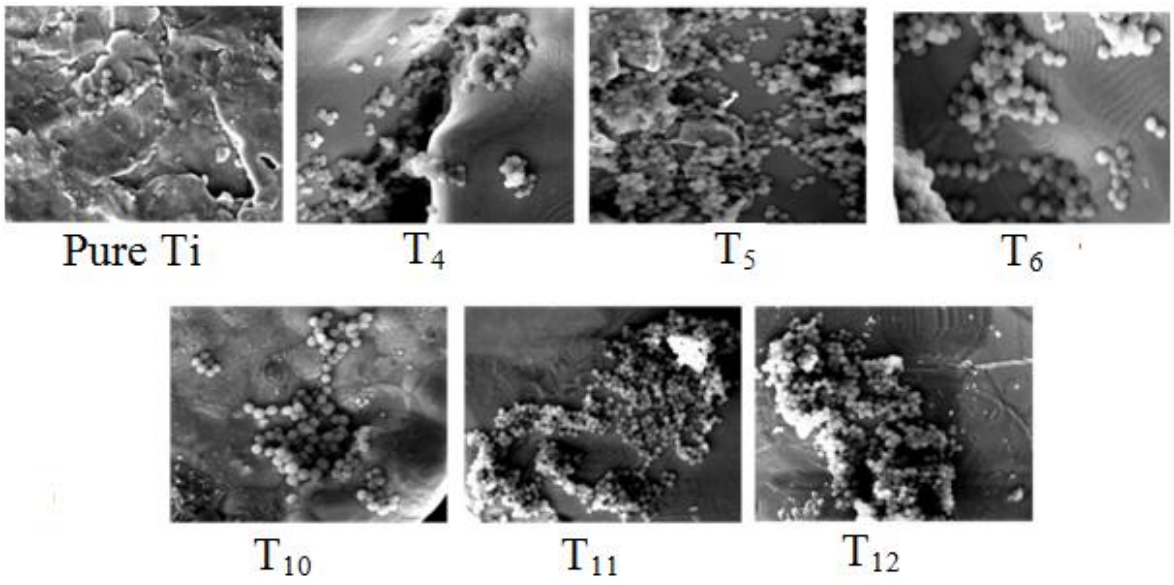

Fig. 5.13. Scanning electron micrograph of various compositions showing biofilm formation by *S.aureu*

5.3.8. Cellular Response

In **Fig. 5.14**, results on cell viability of MC3T3-E1 sub-clone 4 are represented. The results obtained predict the non-toxicity properties in samples of prepared porous Ti-SiO_2 scaffold with the comparative data of pure Ti metal. The rate of cell viability of sample T_{10} is increasing rapidly and it is approximately double when compared to pure Ti sample. Hence it can be concluded that the presence of pores have advantageous on cell viability.

It can be seen from the above results that the porosity of the samples increased as RH wt% increased, and also the percentage of cell viability was increasing from T_4 to T_{12}. Thus we can conclude that cell viability was directly related to porosity of the sample. So from the above observation, it can be concluded that all our formulations have better biocompatibility for orthopaedic application with better mechanical property. Samples of formulation $T_{10,}$ which have been prepared using 20% RH of 180 μm particle size having porosity 25%, show

compressive strength 137 MPa and young's modulus 11 GPa. This composite shows the best biological property and thus, suitable for orthopaedic application.

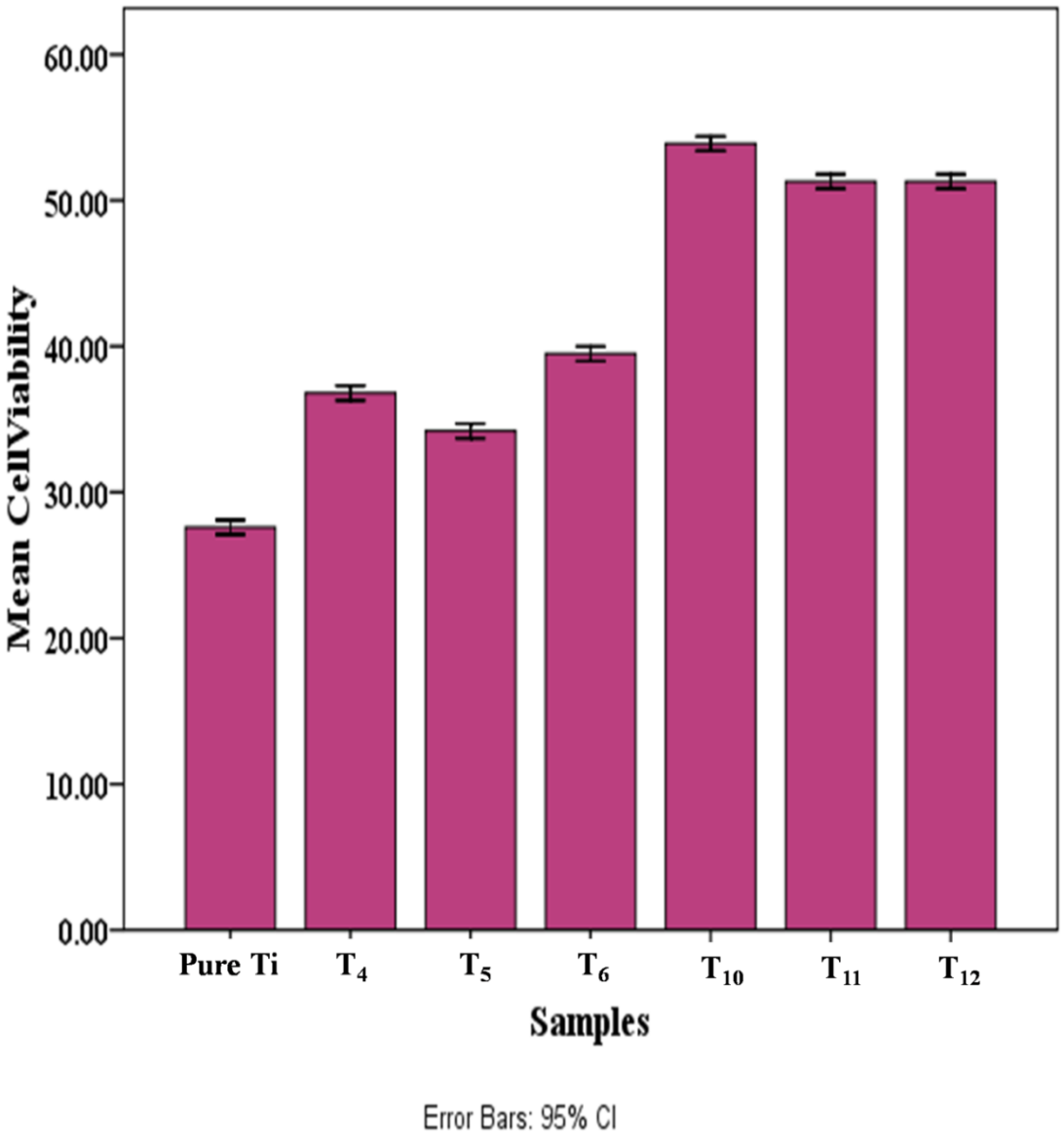

Fig.5.14 Cell viability: The % viability of preosteoblast [cell line MC3T3-E1 subclone 4(ATCC)] on different composites was estimated using MTT assay.

5.4. Conclusion

Porous Ti-SiO_2 composite scaffolds with tailored microstructure and property were successfully developed through powder metallurgy technique using rice husk and sucrose as fugitive material. Porous composite having 15-34% porosity was obtained by varying the amount and size of RH powder in the composition.

The combined use of rice husk and sucrose resulted in the simultaneous incorporation of pores and SiO_2 into the Ti metal matrix in a single step through fugitive burnout by heat treatment in ambient atmosphere. Sintering of green samples in vacuum resulted in formation of porous Ti-SiO_2 composite scaffolds. The presence of SiO_2 reinforcement phase was confirmed from the XRD and EDS analysis. The use of RH as a space holder material creates a scope for fabricating low-cost Ti scaffold along with an advantage of incorporation of silica in the matrix which enhances mechanical and biological properties. Developed porous Ti-SiO_2 composite scaffolds possess Young's modulus in the range 6-15 GPa and compressive strength in the range 117-396 MPa. Also, the developed T_{10} composite porous scaffolds showed the formation of apatite layer when immersed in SBF solution for 7 and 14 days confirming the biocompatibility of porous Ti-SiO_2 scaffold. Higher cell viability was achieved in Ti-SiO_2 porous composites samples as compared to pure Ti metal base scaffolds. The observed results are comparable with the reported results of human cortical bone. Based on experimental results, it can be concluded that the developed porous Ti-SiO_2 composite scaffolds can be suitable for the orthopaedic application.

References

[1] L.L. Hench, Bioceramics: from concept to clinic, Journal of American Ceramic Society. 74 (1991) 1487-1510. DOI: org/10.1111/j.1151-2916.1991.tb07132.x.

[2] W. He, R. Benson, in: K. Modjarrad, S. Ebnesajjad, Handbook of polymer application in medicine and medical devices, ebook ISBN: 978-032-23-2216-96 (2013).

[3] H. Mehboob, S.H. Chang, Application of composites to orthopedic prostheses for effective bone healing: A review, Composite Structures, 118 (2014) 328-341. DOI: 10.1016/j.compstruct.2014.07.052.

[4] G. Ryan, A. Pandit, D.P. Apatsidis, Fabrication methods of porous metals for use in orthopedic applications, Biomaterials. 27 (2006) 2651-2670. DOI: 10.1016/j.biomaterials.2005.12.002.

[5] Y. Dai, Y. Yu, D. Li, K. Yu, D. Jiang, Y. Yan, L. Chen, T. Xiao, Effects of polycaprolactone coating on the biodegradable behavior and cytotoxicity of Mg-6%Zn-10%Ca3(PO4)2 composite in simulated body fluid. 198 (2017) 118-120. DOI: http://dx.doi.org/10.1016/j.matlet.2017.04.002.

[6] K. Xie, L. Wang, Y. Guo, S. Zhao, Y. Yang, D. Dong, W. Ding, K. Dai, W. Gong, G. Yuan, Y. Hao, Effectiveness and safety of biodegradable Mg-Nd-Zn-Zr alloy screws for the treatment of medial malleolar fractures. 27 (2021) 96–100. https://doi.org/10.1016/j.jot.2020.11.007.

[7] D.F. Williams, On the mechanisms of biocompatibility, Biomaterials. 29 (2008) 2941-2953. DOI:10.1016/j.biomaterials.2008.04.023.

[8] D.M. Robertson, L. Pierre, R. Chahal, Preliminary observations of bone ingrowth into porous materials, Journal of Biomedical Material Research. 10 (1976) 335–344. DOI:10.1002/jbm.820100304.

[9] W.C. Head, D.J. Bauk, Jr R.H. Emerson, Ti as the material of choice for cementless femoral components in total hip arthroplasty, Clin Orthop Relat Res. 311 (1995) 85–90.

[10] J.N. Weber, E.W. White, Carbon-metal graded composites for permanent osseous attachment of non-porous metals. Material Research Bulletin, 7 (1972) 1005–16. https://doi.org/10.1016/0025-5408(72)90092-X.

[11] R.M. Pillar, Processing of surgical sintered porous surfaces for tissue to implant fixation International journal of powder metallurgy. 34 (1998) 33.

[12] A.J.T. Clemow, A.M. Weinstein, J.J. Klawitter, J. Koeneman, J. Anderson, Interface mechanics of porous Ti implants, Journal of Biomedical Material Research. 15 (1981) 73–82. https://doi.org/10.1002/jbm.820150111.

[13] E. Tsuruga, H. Takita, H. Itoh, Y. Wakisaka, Y. Kuboki, Pore Size of Porous Hydroxyapatite as the Cell-Substratum Controls BMP-Induced Osteogenesis. Journal of Biochemical. 121 (1997) 317-324. DOI:10.1093/oxfordjournals.jbchem.a021589.

[14] M. Long, H.J. Rack, Ti alloys in total joint replacement-a materials science perspective, Biomaterials. 19 (1998) 1621- 1639. DOI:10.1016/s0142-9612(97)00146-4.

[15] J.W. Qiu, Y. Liu, Y.B. Liu, B. Liu, B. Wang, E. Ryba, Microstructures and mechanical properties of titanium alloy connecting rod made by powder forging process. Material and Design 33(2012) 213–9. DOI:10.1016/j.matdes.2011.07.034.

[16] I. Ibrahim, F. Mohamed, E. Lavernia, Particulate reinforced metal matrix composites – a review. Journal of Material Science 26 (1991)1137–56.

[17] C. Han, Y. Li, X. Wu, S. Ren, X.san, X. Zhu, Ti/SiO_2 composite fabricated by powder metallurgy for orthopedic implant, Material and Design 49 (2013) 76-80. https://doi.org/10.1016/j.matdes.2012.12.060.

[18] X. Zhao, J. You, Y. Xie, H. Cao, X. Liu, Nanoporous SiO_2/TiO_2 composite coating for orthopedic application, Materials Letters. 152 (2015) 53–56. https://doi.org/10.1016/j.matlet.2015.03.067.

[19] Y. Chen, D. Kent, M. Birmingham, A.D. Manshadi, M. Dargusch, Manufacturing of biocompatible porous titanium scaffolds using a novel spherical sugar pellet space holder, Materials letters, 195 (2017) 92-95. DOI: 10.1016/j.matlet.2017.02.092.

[20] K. Mohanta, A. Kumar, O. Prakash, D. Kumar, Processing and properties of low cost macroporous alumina ceramics with tailored porosity and pore size fabricated using RH and sucrose, Journal of European Ceramic Society. 34 (2014) 2401-2412. https://doi.org/10.1016/j.jeurceramsoc.2014.01.024.

[21] K. Mohanta, A. Kumar, O. Prakash, D. Kumar, Low cost porous alumina with tailored microstructure and thermal conductivity prepared using rice husk and sucrose, Journal of American ceramic society. 97 (2014) 1708-1719. https://doi.org/10.1111/jace.12946.

[22] K. Mohanta, A. Kumar, D. Kumar, O. Prakash, Low cost porous alumina with tailored gas permeability and mechanical properties prepared using rice husk and sucrose for filter

applications, Microporous and Mesoporous Materials. (2015) 48-58. https://doi.org/10.1016/j.micromeso.2015.04.004.

[23] K.A. Matori, M.M. Haslinawati, Z.A. Wahab, H.A.A. Sidek, T.K. Ban, W.A.W.A.K Ghani, Producing amorphous white silica from RH, Journal of Basic and Applied Science. 1 (2009) 512-515.

[24] T. Kokubo, H. Takadama, How useful is SBF in predicting in vivo bone bioactivity, Biomaterials. 27(15) (2006) 2907–2915. DOI:10.1016/j.biomaterials.2006.01.017.

[25] W.L. Tham, W.S. Chow, Z.A. Mohd Ishak, Simulated body fluid and water absorption effects on poly(methyl methacrylate)/hydroxyapatite denture base composites, eXPRESS Polymer Letters. 4, 9 (2010) 517–528. DOI: 10.3144/expresspolymlett.2010.66.

[26] B. Bogdan, I. Markovska, Y. Hristov, D. Georgiev, Light-weight materials obtained by utilization of agricultural waste. World Academy of Science Engineering and Technology 64 (2012) 725-728.

[27] S.L. Iconaru, F. Ungureanu, A. Costescu, M. Costache, A. Dinischiotu, D. Predoi, Characterization of sucrose thin films for biomedical applications. Journal of Nanomaterials. (2011)1–7. https://doi.org/10.1155/2011/291512.

[28] R.V. Krishnarao, J. Subrahmanyam, T.J. Kumar, Studies on the formation of black particles in rice husk silica ash. J Eur Ceram Soc 21(2001) 99–104. DOI:10.1016/S0955-2219(00)00170-9.

[29] M.M. Haslinawati, K.A. Matori, Z.A. Wahab, H.A.A. Sidek, A.T. Zainal, Effect of temperature on ceramic from rice husk ash. International Journal of Basic and Applied Science 9(2009) 22–5.

[30] C.H. Schilling, S.B. Biner, H. Goel, J. Jane, Plastic shaping of aqueous alumina suspension with sucrose and maltodextrin additives. Journal of Environmental Polymer Degradation 3(1995) 153–240.

[31] I.H. Oh, N. Nomura, N. Masahashi, Shuji Hanada, Mechanical properties of porous titanium compacts prepared by powder sintering. Scripta Materialia 49(2003) 1197-1202. https://doi.org/10.1016/j.scriptamat.2003.08.018.

[32] W. Xue. B.V. Krishna, A. Bandyopadhyay, S. Bose, Processing and biocompatibility evaluation of laser processed porous titanium. Acta Biomaterialia 3(2007) 1007-1018. DOI:10.1016/j.actbio.2007.05.009.

[33] X.S. Wang, Z.L. Lu, L. Jia, J.X. Chen, Preparation of porous Titanium materials by powder sintering process and use of space holder technique. Journal of iron and steel research International 24 (2017) 97-102, DOI:10.1016/S1006-706X(17)30014-6.

[34] D. Wang, Q. Li, M. Xu, G. Jiang, Y. Zhang, G. He, A novel approach to fabrication of three-dimensional porous titanium with controllable structure. Material Science and Engineering C 71 (2017) 1046-1051. DOI: 10.1016/j.msec.2016.11.119.

[35] A. Nouri, D. Hodgson, C. Wen, in: A. Mukherjee, Biomimetics learning from nature, eBook (PDF) ISBN: 978-953-51-4555-4, 2010, pp. 415- 450, DOI: 10.5772/198

[36] S.C.P. Cachinho, R.N.Correia, Titanium scaffolds for osteointegration: mechanical, in vitro and corrosion behavior. Journal of Material Science Materials in Medicine. 19 (2008) 19451–457. DOI:10.1007/s10856-006-0052-7.

[37] Y. Chen, X. Zheng, H. Ji, C. Ding, Effect of Ti–OH formation on bioactivity of vacuum plasma sprayed titanium coating after chemical treatment. Surface and Coating Technology. 202 (2007) 494-498. DOI: https://doi.org/10.1016/j.surfcoat.2007.06.015

[38] C. R. Arciola, D. Campoccia, L. Montanaro, Implant Infections: Adhesion, Biofilm Formation and Immune Evasion, Nature Reviews Microbiology. Nature Publishing Group (2018), 397–409. https://doi.org/10.1038/s41579- 018-0019-y.

[39] L. E. Nicolle, Catheter Associated Urinary Tract Infections, Antimicrobial Resistance and Infection Control, 3 (1), 23 (2014). https://doi.org/10.1186/2047-2994-3-23.